The Linnean Society of London ZOOLOGICAL Journal of the Linnean Society

Zoological Journal of the Linnean Society, 2010, **158**, 231–243. With 7 figures

Morphology and morphogenesis of a new marine hypotrichous ciliate (Protozoa, Ciliophora, Pseudoamphisiellidae), including a report on the small subunit rRNA gene sequence

LIQIONG LI[1], WEIBO SONG[1]*, KHALED A. S. AL-RASHEID[2], ALAN WARREN[3], ZICONG LI[1], YUAN XU[1] and CHEN SHAO[1]

[1]*Laboratory of Protozoology, KLM, Ocean University of China, Qingdao 266003, China*
[2]*Zoology Department, King Saud University, P.O. Box 2455, Riyadh 11451, Saudi Arabia*
[3]*Department of Zoology, Natural History Museum, Cromwell Road, London SW7 5BD, UK*

Received 4 June 2008; accepted for publication 5 November 2008

The morphology and morphogenesis of a new marine hypotrichous ciliate ***Pseudoamphisiella elongata* sp. nov.** isolated from mussel-farming waters near Qingdao, China, are described based on living and protargol-impregnated specimens. Morphologically, the new species can be distinguished from its known congeners by its elongate body shape, narrow oral field, having fewer dorsal kineties and caudal cirri, more marginal cirri, and differentiated pretransverse cirri. The identification as a new species is firmly supported by the sequences of the small subunit ribosomal rRNA (SSU rRNA) gene, compared with other known *Pseudoamphisiella* species, and the phylogenetic analysis. The morphogenetic characteristics can be summarized as follows: (1) the parental adoral zone of membranelles and undulating membranes are entirely rebuilt by the oral primordium, which develops *de novo* in the outermost region of the cortex; (2) the oral primordium in the opisthe and the frontoventral–transverse (FVT) anlagen in both dividers are formed independently on the cell surface; (3) an 'extra' marginal anlage originates to the right of the right marginal anlage, and develops into two or three 'extra' marginal cirri; (4) the FVT anlagen develop in the primary mode, and the last FVT streak contributes two migratory cirri (frontoterminal cirri), which are probably resorbed; (5) the right marginal anlagen in both dividers occur close together, independent of the old structure.

doi: 10.1111/j.1096-3642.2009.00546.x

ADDITIONAL KEYWORDS: hypotrichida – infraciliature – new species – ***Pseudoamphisiella elongata* sp. nov.** – stomatogenesis – taxonomy.

INTRODUCTION

Pseudoamphisiella is a well-defined genus that includes three known species, namely *Pseudoamphisiella lacazei* (Maupas, 1883) Song, 1996, *Pseudoamphisiella alveolata* (Kahl, 1932) Song & Warren, 2000, and *Pseudoamphisiella quadrinucleata* Shen *et al.*, 2008, all of which have been investigated using modern methods, including living observations, silver impregnation, and small subunit ribosomal rRNA (SSU rRNA) gene sequencing (Song, 1996; Song, Warren & Hu, 1997; Song & Warren, 2000; Berger, 2006; Hu & Suzuki, 2006; Shao *et al.*, 2006; Shen *et al.*, 2008). Furthermore, the first two species have been investigated morphogenetically, although details for *P. quadrinucleata* remain unknown (Song, 1996; Song & Warren, 2000).

In 2007, we isolated a hypotrich ciliate from coastal waters off Qingdao, China. Uniprotistan cultures were established, and detailed investigations of its morphology, morphogenesis, and SSU rRNA gene sequence were carried out. The results demonstrate it should be a new species within the genus *Pseudoamphisiella*.

*Corresponding author. E-mail: wsong@ouc.edu.cn

MATERIAL AND METHODS

Collection and cultivation

Pseudoamphisiella elongata sp. nov. was collected on 27 November 2007 from open mussel-farming waters of the Yellow Sea coast near Qingdao (36°08′N, 120°43′E), where the salinity was 29–31‰, the water temperature 8 °C and pH 8.0. Glass slides were used as artificial substrates for collecting the ciliates. The slides were left immersed at a depth of 1 m for 15 days to allow colonization by ciliates to occur. Isolated specimens were maintained in Petri dishes for about 7 days as raw, uniprotistan cultures (water temperature ~18 °C, salinity ~30‰; Lin *et al.*, 2008).

Morphology and morphogenesis

Observations on live specimens were undertaken using an oil immersion objective and interference contrast microscopy. Protargol staining (Wilbert, 1975) was used to reveal the infraciliature and nuclear apparatus.

Drawings of impregnated specimens were performed at a magnification of 1250× with the help of a camera lucida. Measurements were carried out with an ocular micrometer. To distinguish the changes during morphogenesis and reorganization, parental cirri are depicted with outlines, whereas new cirri are shaded in black (Li *et al.*, 2008). Drawings of live specimens are based on *in vivo* observation and photomicrographs. The terminology and systematics follow that of Berger (2006) and Lynn & Small (2002), respectively.

Genomic DNA extraction, PCR amplification, sequencing, and analyses

Genomic DNA extraction, PCR amplification, and SSU rDNA region cloning and sequencing of *P. elongata* sp. nov. were performed according to the method described by Shang, Song & Warren (2003). Two primers were used: 82F, 5′-GAAACTGCGAATGGCTC-3′; 16s-R, 5′-TGATCCTTCTGCAGGTTCACCTAC-3′. The nucleotide sequences used in this paper are available from the GenBank database. *Protocruzia contrax* (Mansfield, 1923) Kahl, 1932 (DQ190467) was selected as the outgroup species. The PHYLIP package, v3.75c (Felsenstein, 1995), was used to calculate the genetic distances among the four *Pseudoamphisiella* species. Phylogenetic analyses were performed according to the method described by Yi *et al.* (2008).

RESULTS

Order Hypotrichida Stein, 1859

Family Pseudoamphisiellidae Song *et al.*, 1997

Genus *Pseudoamphisiella* Song, 1996

***Pseudoamphisiella elongata* sp. nov.**

(Figs 1, 2; Table 1)

Diagnosis: Elongated marine *Pseudoamphisiella*, *in vivo* 160–240 μm × 30–40 μm, with conspicuous extrusomes within outer alveolar layer, 25–44 macronuclear nodules, and 6–17 micronuclei. On average, 44 adoral membranelles; two buccal and three frontal cirri; one row of 16–21 strong transverse cirri that

Table 1. Morphometric characterization of ***Pseudoamphisiella elongata* sp. nov.**

Character	Min.	Max.	Mean	SD	*N*
Length of body	160 μm	224 μm	192.7 μm	15.4 μm	30
Width of body	48 μm	68 μm	56.5 μm	5.4 μm	30
Length of adoral zone	40 μm	64 μm	48.2 μm	6.4 μm	30
Membranelles	39	49	44.3	1.9	30
Buccal cirri	2	2	2	0	30
Frontal cirri	3	3	3	0	29
Left midventral cirri	13	17	15.5	1.1	29
Right midventral cirri	15	21	18.1	1.6	29
Left marginal cirri	26	45	38.1	4.6	28
Right marginal cirri	28	36	31.6	2.1	28
Transverse cirri	16	21	19.1	1.4	29
Pretransverse cirri	2	3	2.4	0.5	24
Caudal cirri	6	7	6.9	0.3	27
Dorsal kineties	6	7	6.9	0.3	28
Macronuclear nodules	25	44	33.4	6.1	29
Micronuclei	6	17	11.8	2.5	23

Data based on protargol-stained specimens.

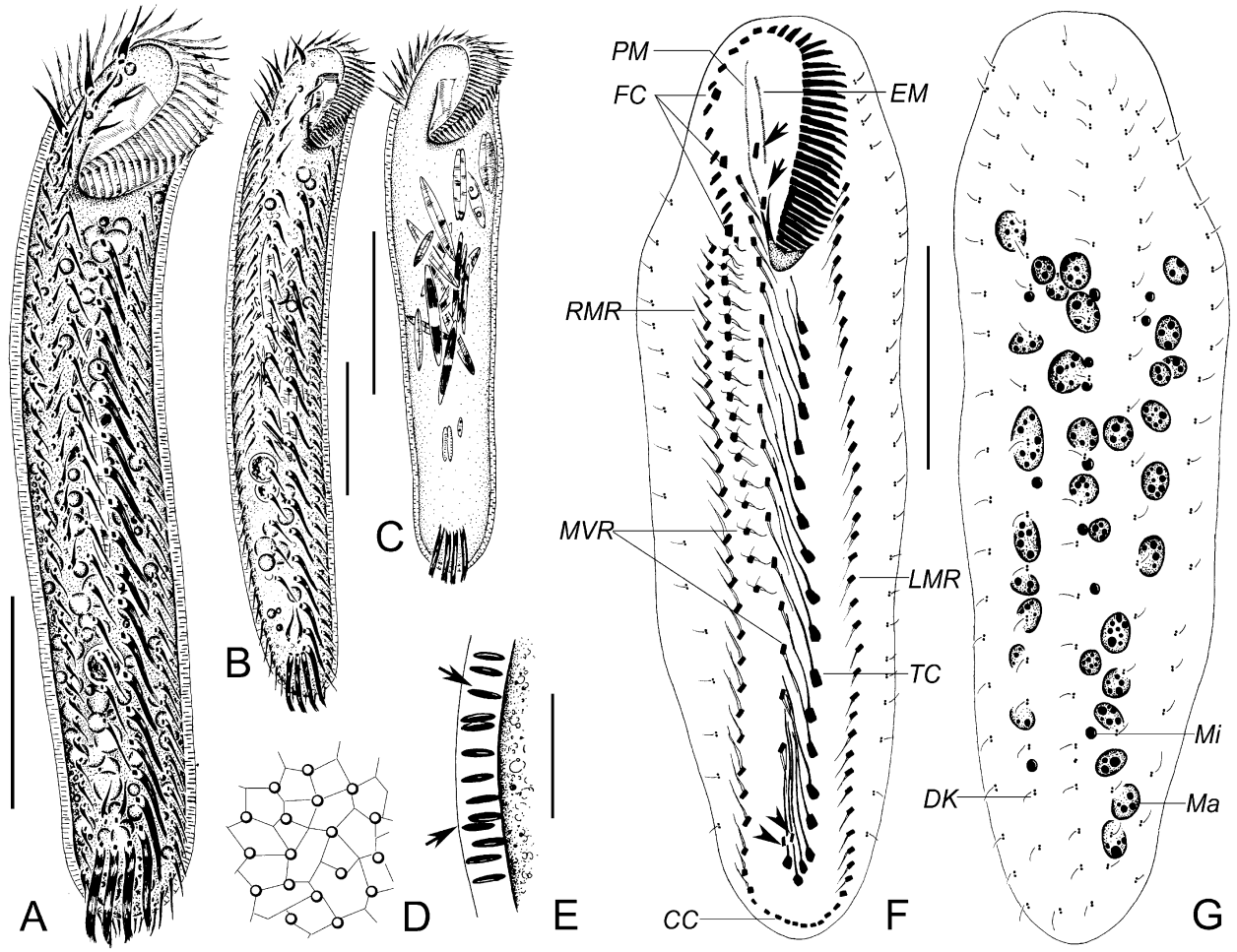

Figure 1. Morphology of ***Pseudoamphisiella elongata*** **sp. nov.** from living observation (A–E) and after protargol impregnation (F–G). A, ventral view of a typical individual; B, ventral view of a slimmer individual; C, ventral view, note the ingested pennate diatoms; D, E, portion of cortex (top and side view), showing the polygonal-shaped alveoli and the rod-shaped extrusomes (arrows); F, ventral view of infraciliature, arrowheads indicate two fine pretransverse cirri; G, dorsal view of the same specimen as shown in (F), showing the macronuclear nodules, micronuclei, and dorsal kineties. Abbreviations: CC, caudal cirri; DK, dorsal kineties; EM, endoral membrane; FC, frontal cirri; LMR, left marginal row; Ma, macronucleus; Mi, micronucleus; MVR, midventral row; PM, paroral membrane; RMR, right marginal row; TC, transverse cirri. Scale bars: 50 μm in A, B, C, F, G; 10 μm in E.

extends anteriorly almost to the proximal end of the adoral zone of membranelles (AZM); two or three fine pretransverse cirri; two widely separated ventral rows comprising between 16 and 18 cirri, respectively; 26–45 and 28–36 cirri in left and right marginal rows, respectively; six or seven caudal cirri; six or seven dorsal kineties.

Type locality: Mariculture waters of the Yellow Sea coast at Qingdao, China (36°08′N; 120°43′E).

Type specimens: One holotype slide of protargol-impregnated specimens is deposited in the Natural History Museum, London, UK, with registration no. 2008:5:14:1. One paratype slide is deposited in the Laboratory of Protozoology, Ocean University of China (OUC), Qingdao, China, registration no. LLQ-20071127-01.

Etymology: The species name *elongata* (Latin adjective, meaning elongated or stretched) refers to the elongate body shape.

Description: Cells are mostly 200 μm × 30 μm *in vivo*, with a length to width ratio ranging roughly from 5 : 1 to 7 : 1. Body elongate, slender, and more or less cephalized; posterior end only slightly narrowed (Figs 1A, B; 2A, D). Cell flexible and slightly

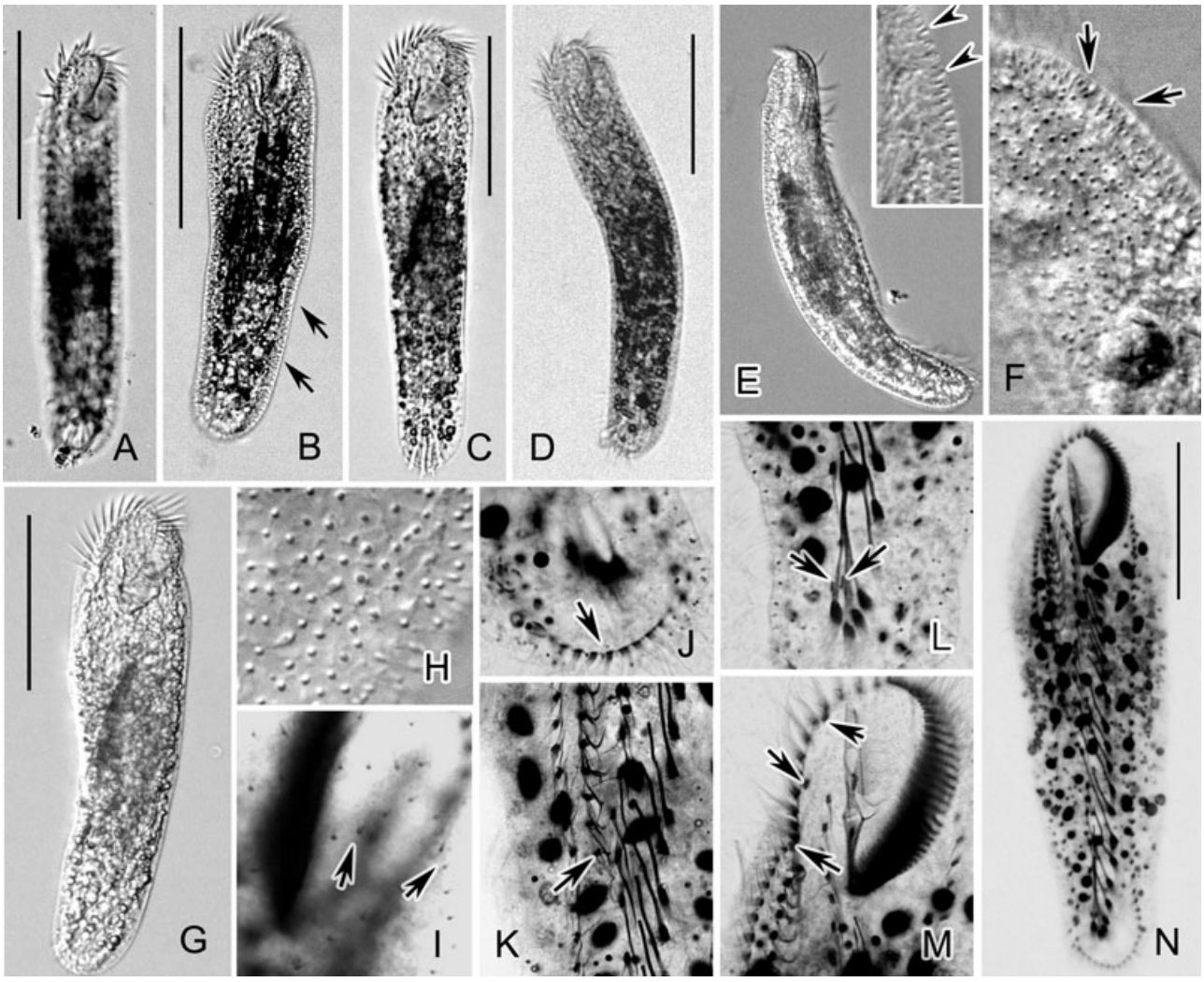

Figure 2. Photomicrographs of ***Pseudoamphisiella elongata* sp. nov.** from life (A–H) and after protargol impregnation (I–N). A–D, ventral views of different individuals, arrows mark the pellicular alveolus; E, lateral view, the inset shows part of the cortex, and the arrowheads indicate the rod-shaped extrusomes; F, portion of cortex (dorsolateral view), arrows indicate the extrusomes; G, outline shape of a stationary individual; H, dorsal view of cortex, showing the polygonal-shaped alveoli; I, dorsal view, arrows mark the dorsal kineties; J, caudal portion, the arrow indicates the caudal cirri; K, middle portion of cell, ventral view, the arrow marks the end of the right midventral row; L, posterior end of body, ventral view, the arrows indicate the two fine pretransverse cirri that can be easily overlooked; M, anterior part of body, ventral view, arrows indicate the frontal cirri; N, ventral infraciliature. Scale bars: 100 μm in A, B; 50 μm in C, D, G, H.

contractile, making it a little shorter when stationary than when moving (Fig. 2B, G). Body margins generally straight and parallel. Outline shape variable, depending on nutritional status; starving individuals were widest in the buccal field (Figs 1C, 2C). Dorsoventrally flattened about 1 : 3 (Fig. 2E). Buccal field characteristically short and narrow, about 15% of body length *in vivo* (Fig. 1A, B).

Pellicular alveolar layer clearly observed *in vivo*, about 3–4-μm thick, with densely arranged rod-shaped extrusomes perpendicular to pellicle (Figs 1E arrows, 2B arrows, 2E inset, 2F). When viewed dorsally, the alveolar layer is seen to have an irregular polygonal structure (Figs 1D, 2H).

Cytoplasm colourless, whereas ingested food (e.g. pennate diatoms) usually makes the cell opaque when observed at lower magnifications (Fig. 2A, B, D). Contractile vacuole not observed, possibly absent. Between 25 and 44 macronuclear nodules (Ma), spherical to slightly oval in shape; between 6 and 17 micronuclei (Mi), spherical, about 3 μm in diameter (Figs 1G, 2N).

Locomotion is typically achieved by rapid and continuous crawling on debris or on the bottom of the

Petri dish. Occasionally *P. elongata* sp. nov. specimens remain still for long periods, until they are disturbed.

The distal end of the AZM curves posteriorly onto the right side towards the buccal cavity. The longest membranelle base is about 12-μm wide, with those in the distal (right) portion of the AZM distinctly shorter than those in proximal (left) portion. The paroral membrane (PM) is shorter than the endoral membrane (EM), but they do not cross each other (Figs 1F, 2M).

Most of the somatic cirri are relatively fine and are about 15-μm long. Three slightly enlarged frontal cirri (FC) are situated along the distal portion of the AZM. The posteriormost FC are positioned between the anterior end of the right marginal row and the distal end of the AZM (Figs 1F, 2M arrows). Two medium-sized buccal cirri (BC) are located between the PM and the EM (arrows in Fig. 1F). The left midventral row is long, starting near the undulating membranes (UM) and terminating at the posterior fifth of the body length (Figs 1F, 2N). The right midventral row (RMVR) is composed of densely arranged cirri, anteriorly terminating around the distal end of the AZM, and extending posteriorly to between three-fifths and two-thirds of the body length (Figs 1F, 2K arrow).

About 20 highly developed transverse cirri (TC), ~20 μm long, are arranged in a J-shaped row that extends anteriorly to about the level of the cytostome (Figs 1F, 2N). Two fine pretransverse cirri (PTC) are situated close to the posterior end of the TC (Figs 1F arrowheads, 2L arrows). The left and right marginal rows (LMR, RMR) have 26–45 and 28–36 cirri, respectively; the ends of the marginal rows are confluent with caudal cirri at the posterior end of cell, and hence it is difficult to distinguish where the marginal rows terminate (Figs 1F, 2J arrow). Strong fibrils are associated with almost all of the somatic cirri, as revealed by protargol impregnation (Figs 1F, 2N).

Six or seven dorsal kineties (DK) extend along the whole length of the body, with dorsal cilia of about 5-μm long (Figs 1G, 2I arrows).

Divisional morphogenesis (Figs 3–6)

The earliest stage observed was the appearance of the oral primordia (OP), with several streaks formed between transverse cirri and the left midventral row. Noticeably, the OP in both the proter and opisthe form in the outermost region of the cortex (Figs 3A arrows and double-arrowhead, 5A). The parental oral apparatus and all old cirri, including the fibres, remain intact indicating that the parental structures do not participate in the formation of the OP. With the proliferation of basal bodies, the middle regions of the primary streaks (Fig. 3A, arrowheads) appear to rupture, to form the secondary frontoventral–transverse (FVT) anlagen of the proter (Fig. 3B). Remarkably, the right marginal row anlagen (RMA) in both dividers originate very close together, independently of the parental right marginal row (Fig. 3B arrows).

In the next stage, the posterior portion of the parental AZM and the undulating membranes begin to disorganize. The FVT-anlagen in both dividers become arranged as ladder-like structures, each of which comprises about 20 streaks (arrow in Fig. 3C). By this stage, the development of membranelles in the right anterior part of this area has already begun, and the left marginal anlagen develop within the old structure (Figs 3C double-arrowheads, 5C arrowheads, 5F arrows). The dorsal kineties develop from two anlagen within each parental kinety, which by now consist of short, close-set rows of basal bodies (Fig. 3C).

As the construction of new membranelles continues, the left marginal row anlagen derived from several dedifferentiated parental cirri appear within the old structure (Fig. 3D). The development of the somatic ciliature in both dividers is similar and takes place at about the same time. The new adoral membranelles and the undulating membrane anlage (UMA) differentiate in a posterior direction. Two sets of basal bodies (the 'extra' anlagen) appear at the posterior right of the RMA in each divider (arrowheads in Fig. 3D). By this time, the macronuclear nodules are somewhat expanded with no recognizable replication band, and the micronuclei have completed the process of fusion (Fig. 3E).

Slightly later, the enlarged macronuclear nodules begin to move towards the centre of the cell (Figs 3F, 5D). The UMA starts aggregating into the undulating membranes. The UM anlage remains as a single unit until the late stage, and then splits longitudinally to form the paroral and endoral membranes. Division continues with the complete formation of the FVT cirral anlagen to the right of the OP, within which each streak seems to break into several segments (Fig. 3F). Meanwhile, a single segment is derived from the UMA, which will become the leftmost frontal cirrus for each divider.

As the morphogenetic process proceeds further, each of the FVT-streaks, except the last two, develops into three cirri that are placed in three oblique rows (Fig. 3G). Each of the last two streaks generates four cirri. Two macronuclear masses appear, along with a number of expanded micronuclei (Fig. 3G, inset; Fig. 5E).

Eventually, the macronuclear nodules fuse into a single mass, with several enlarged micronuclei attached to it (Fig. 4B). At the same time the two anteriormost cirri from the last FVT-streak begin to

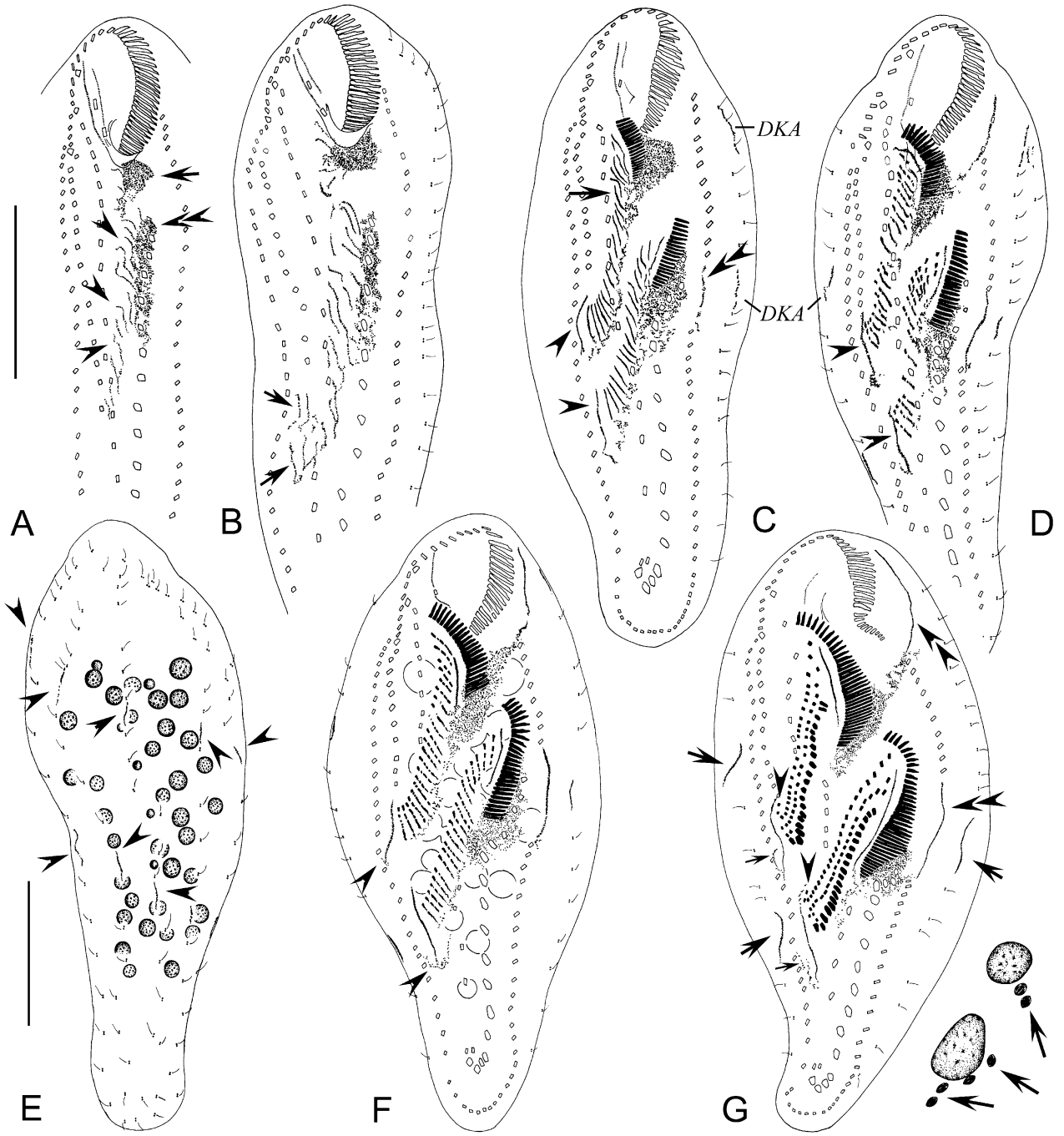

Figure 3. ***Pseudoamphisiella elongata*** **sp. nov.** after protargol impregnation, showing early to middle stages of morphogenesis. A, ventral view of an early stage divider, note the oral primordium in the proter (arrow) and opisthe (double-arrowheads), arrowheads indicate the primary frontoventral–transverse (FVT) cirral anlagen; B, ventral view, showing the early stage, arrows indicate the primary right marginal row anlagen; C, ventral view of an early divider, arrow marks the FVT-anlagen, arrowheads indicate the right marginal row anlagen, the double-arrowheads show the left marginal row anlagen in the opisthe; D, E, ventral and dorsal views of the same individual, arrowheads in D and E indicate the right marginal row anlagen and dorsal kineties anlagen, respectively; F, a slightly late divider, arrowheads indicate the extra anlagen; G, middle-stage divider, showing the dorsal kineties anlagen (arrows), the left marginal row anlagen (double-arrowheads), two migratory cirri derived from the last FVT-streak (arrowheads), and the hook-like extra anlagen; the inset shows the macronuclear nodules, and arrows mark the micronuclei. DKA: dorsal kineties anlagen.

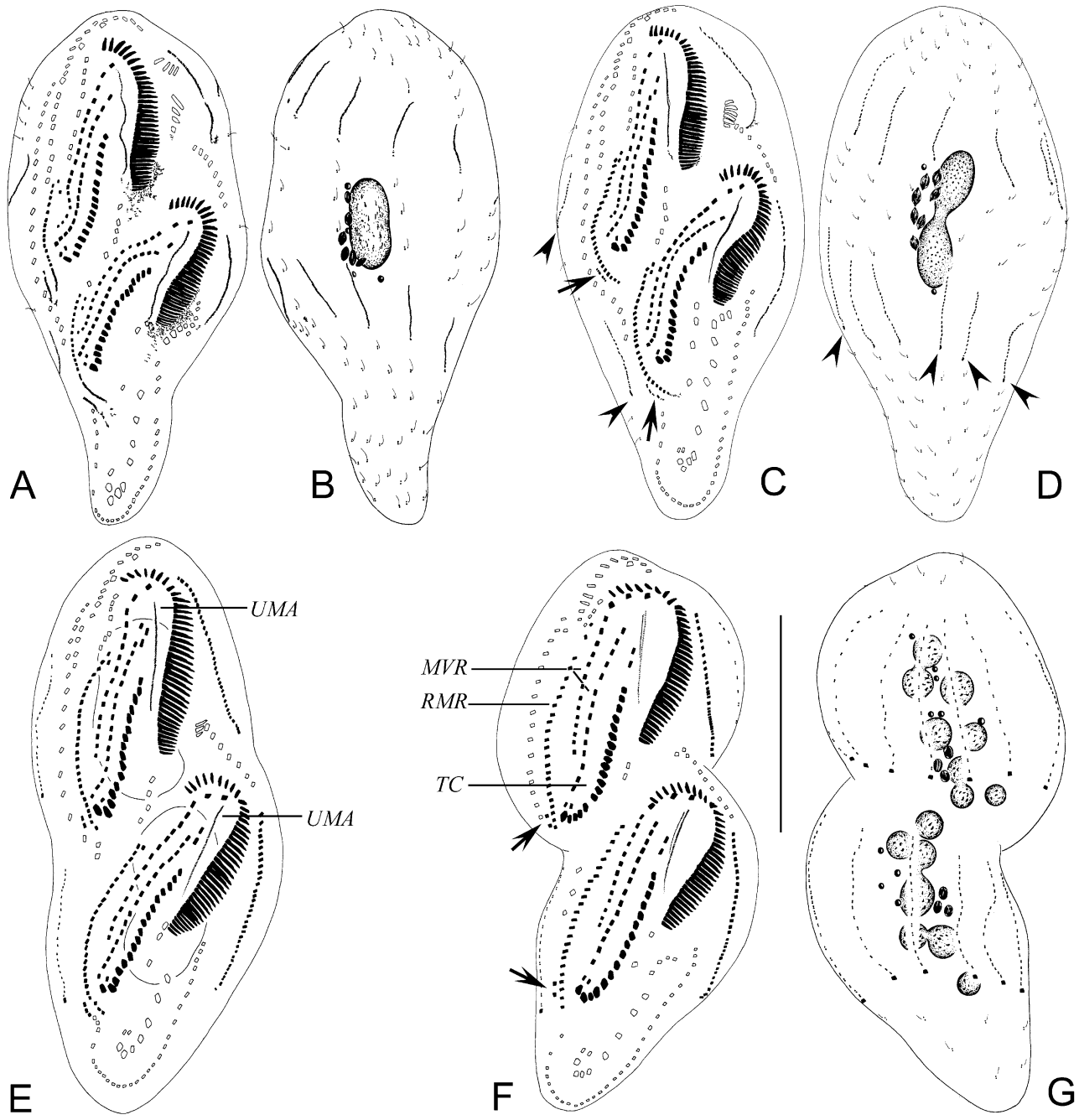

Figure 4. ***Pseudoamphisiella elongata*** **sp. nov.** in the middle and late stages of morphogenesis, after protargol impregnation. A, B, ventral and dorsal views of the same specimen in the middle stage, showing the development of cirri and the single macronuclear mass; C, D, ventral and dorsal views of a late divider (same specimen), arrows indicate the differentiation of the extra anlagen, and arrowheads show the single caudal cirrus that develops from the posterior end of each dorsal kinety; E, ventral view of a late divider, note the newly built cirri; F, G, ventral and dorsal views of a very late divider, arrows indicate the newly formed extra right marginal cirri. Abbreviations: MVR, midventral row; RMR, right marginal row; TC, transverse cirri; UMA, undulating membrane anlagen. Scale bar: 60 μm.

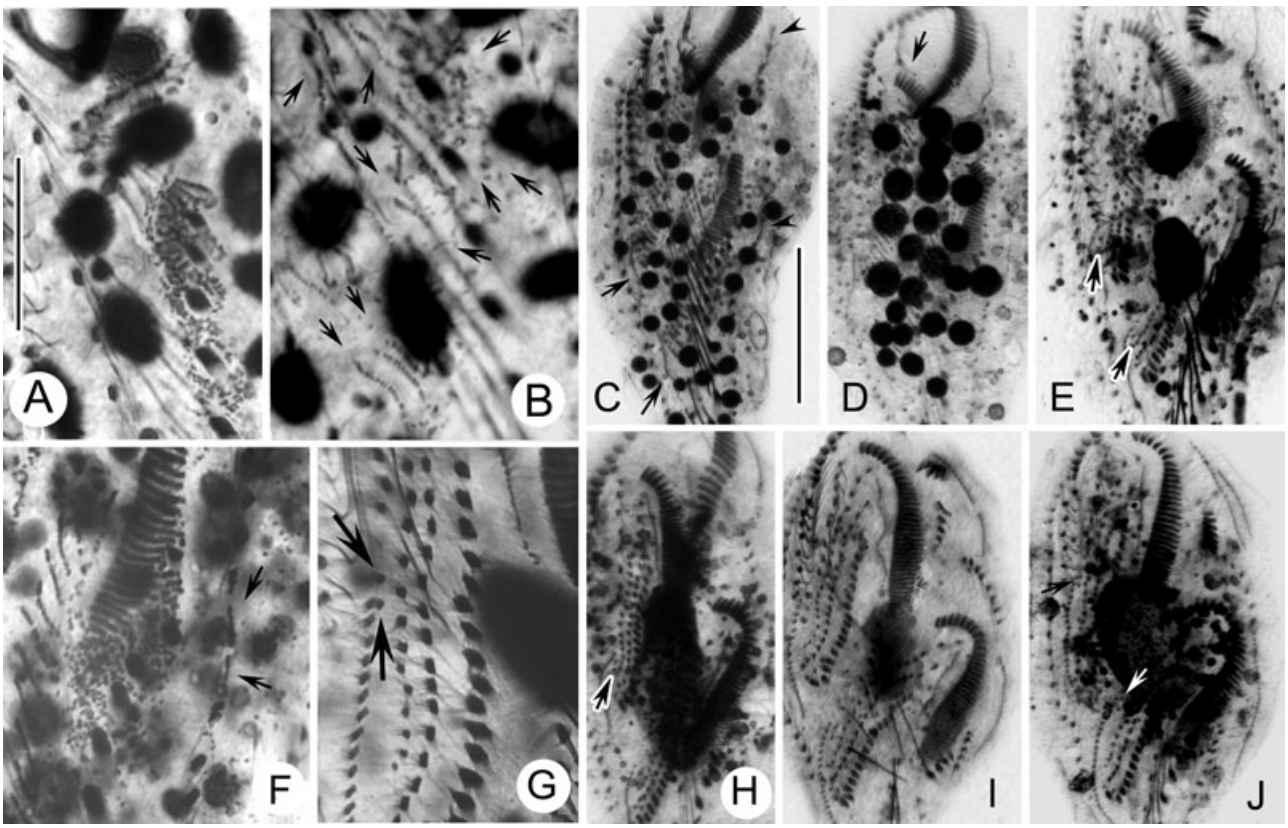

Figure 5. Photomicrographs of morphogenesis in ***Pseudoamphisiella elongata*** **sp. nov.** after protargol impregnation. A, middle part of cell, ventral view, showing the oral primordium for both dividers, and the undifferentiated parental structures; B, ventral view, arrows indicate the primary frontoventral–transverse (FVT) anlagen; C, ventral view of an early divider, arrowheads and arrows mark the left and right marginal row anlagen, respectively; D, a slightly later stage, note the merging of the macronuclear nodules, the arrow indicates the disaggregating of the old undulating membranes; E, ventral view of a middle-stage divider, arrows indicate the two migratory cirri derived from the last FVT cirral anlagen; F, middle portion of cell, ventral view, arrows mark the left marginal row anlagen in the opisthe; G, ventral view, arrows denote two migratory cirri derived from the last FVT cirral anlagen; H–J, ventral views of three specimens at slightly differing middle stages, the arrows in (H) and (J) indicate two migratory cirri derived from the last FVT cirral anlagen. Scale bars: 15 μm in A; 50 μm in C.

migrate anteriad towards the top of the newly built right marginal row (Figs 4A, 5H arrow, 5J arrows).

During the subsequent stages the formation of the AZM in both dividers is completed, and most of the old oral apparatus and somatic organelles are disaggregated (Fig. 4C–G). The new cirri generated from the FVT-streaks migrate to their final positions becoming the frontal, buccal, midventral, pretransverse, and transverse cirri, respectively. Noticeably, the two anteriormost cirri from the last streak finally migrate close to the top of the newly built right marginal row, becoming frontoterminal cirri that eventually appear to be resorbed (Fig. 4A, C, E, F). The 'extra' anlagen give rise to two or three cirri that migrate to the posterior end of the right marginal row in both dividers (arrows in Figs 4C, F, 6A). The UMA split in both the proter and the opisthe, forming the paroral and endoral membranes (Fig. 4F). The new cirral rows begin to extend as the cell elongates, and migrate to form the mature cortical pattern. The dorsal kineties anlagen stretch in both directions to replace the old structures (Figs 4F, 6B arrows). A single caudal cirrus develops from the posterior end of each dorsal kinety: these cirri migrate caudally and form a row that is confluent with the posterior ends of the marginal rows (Fig. 4D arrowheads, G). The macronuclear nodules and micronuclei begin to divide in the usual way (Fig. 6E–K).

Eventually, the daughter cells separate and, with the completion of the cytostome, become trophic cells.

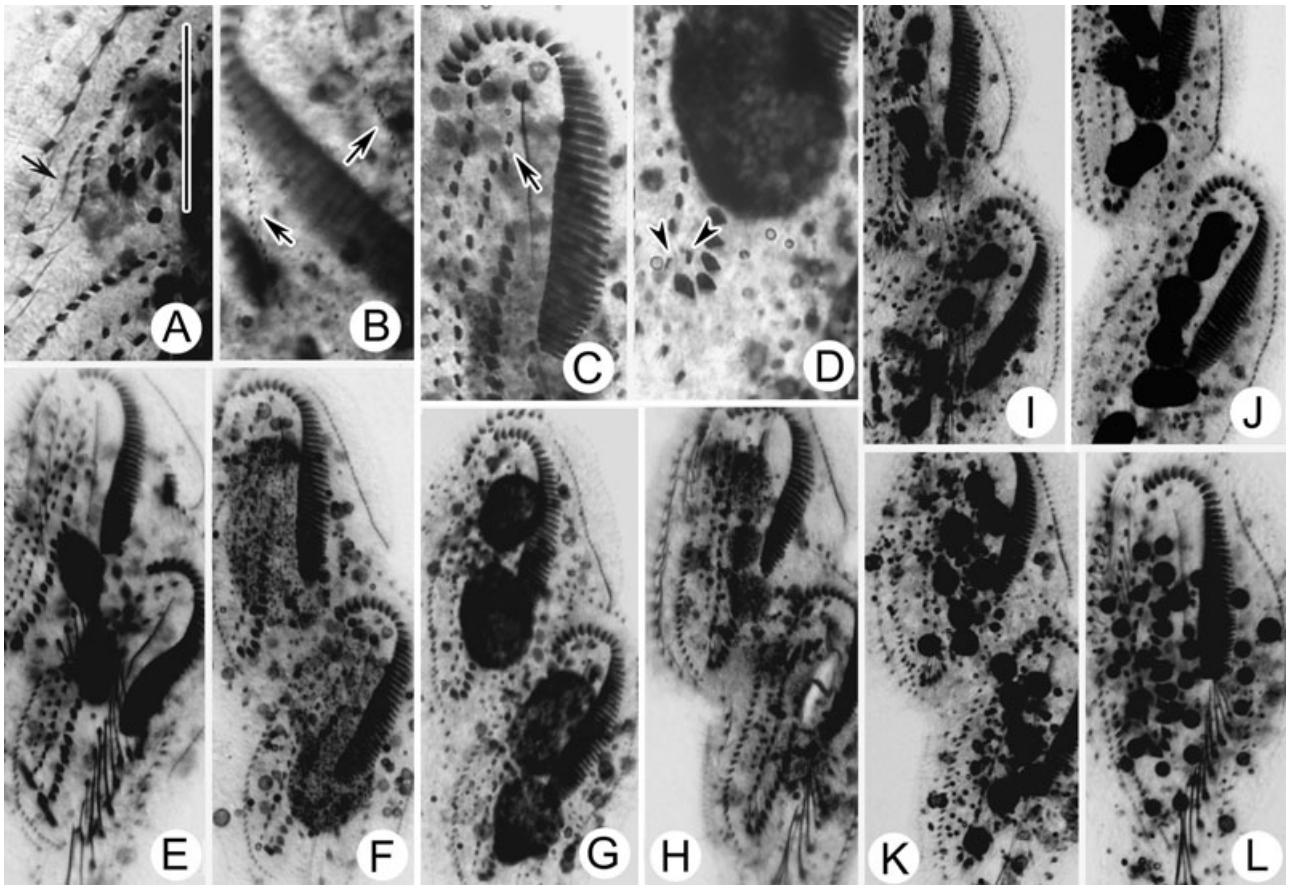

Figure 6. Photomicrographs of morphogenesis in ***Pseudoamphisiella elongata* sp. nov.** after protargol impregnation. A, ventral view, the arrow indicates the extra anlage adjacent to the right marginal row anlage; B, dorsal view, arrows denote the dorsal kineties anlagen; C, ventral view of opisthe in late stage, the arrow marks two buccal cirri; D, ventral view, arrowheads denote the pretransverse cirri; E–K, ventral views of middle to late stage dividers, showing the migration of all ciliary organelles and the division of the macronuclei; L, ventral view of a reorganizer at a late stage. Scale bars: 25 μm in A; 60 μm in E.

SSU rRNA GENE SEQUENCE ANALYSIS (FIG. 7; TABLE 2)

The SSU rRNA gene sequence of *P. elongata* sp. nov. has been deposited in the GenBank database, with accession number EU571944.

The genetic distance between *P. elongata* sp. nov. and its congeners ranges from 0.0473 to 0.0564, which is larger than the distance among the three known species (Table 2). These data, along with the comparisons of the nucleotide sequences of the SSU rRNA gene regions (Fig. 7A), indicate that *P. elongata* sp. nov. is clearly separate from its congeners, thus supporting its validity as a new species of *Pseudoamphisiella*.

Both methods of phylogenetic analyses (maximum likelihood, ML, and Bayesian inference, BI) resulted in congruent topologies and were thus combined into a single tree (Fig. 7B). *Pseudoamphisiella* formed a well-supported group with full bootstrap value in the ML tree, and maximum posterior probability in the Bayesian analysis. Within the genus *Pseudoamphisiella*, four species are clustered into two clades: *P. elongata* sp. nov. was grouped with *P. lacazei* with high support (90% ML, 1.00 BI).

Table 2. The genetic distances between the SSU rRNA gene sequences of four *Pseudoamphisiella* species using the PHYLIP package based on the two-parameter model (Kimura, 1980)

	P. elongata	*P. alveolata*	*P. lacazei*
P. alveolata	0.0564	–	–
P. lacazei	0.0473	0.0445	–
P. quadrinucleata	0.0558	0.0053	0.04207

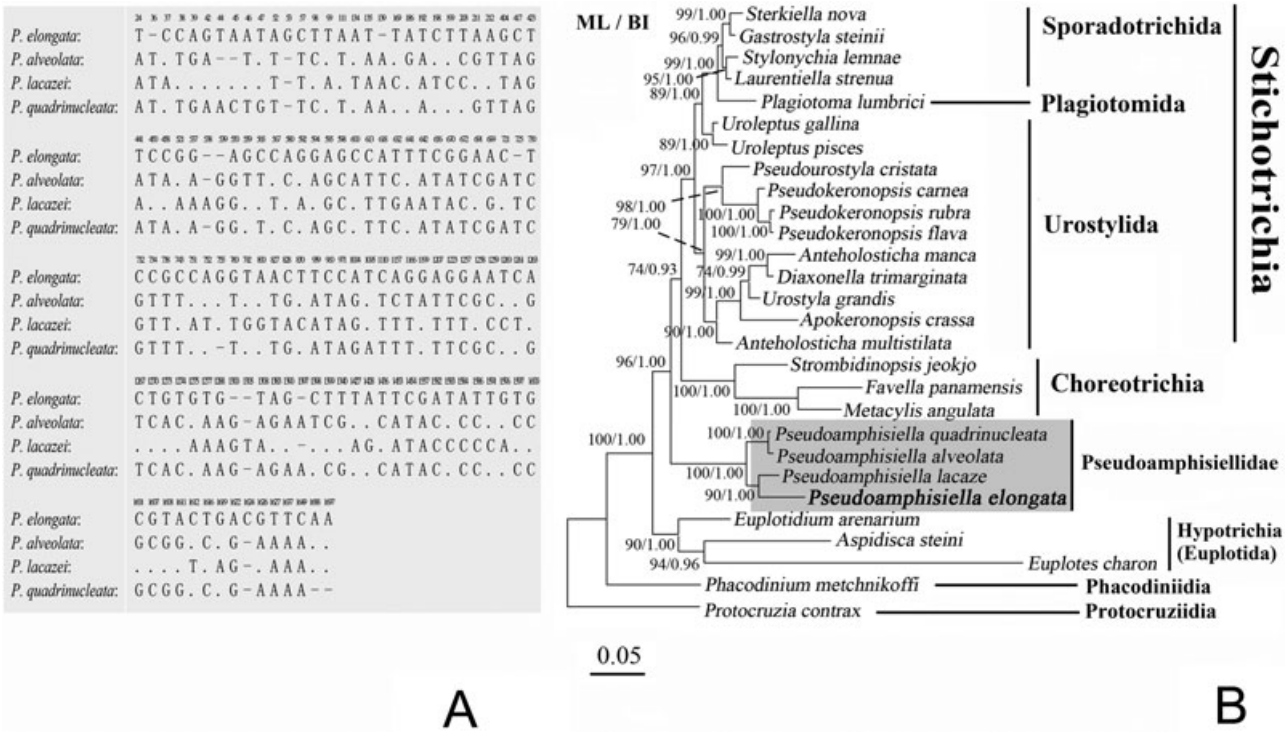

Figure 7. A, small subunit (SSU) rRNA gene sequence of ***Pseudoamphisiella elongata* sp. nov.** aligned with the sequences of *Pseudoamphisiella alveolata*, *Pseudoamphisiella lacazei*, and *Pseudoamphisiella quadrinucleata*. The numbers above the lines indicate the nucleotide numbers. The differences in sequence lengths were compensated for by introducing alignment gaps (–) in the sequences. Matched sites are marked with dots. B, phylogenetic tree of SSU rRNA sequences showing the positions of *Pseudoamphisiella* found with maximum-likelihood (ML) analysis, applying the GTR+G+I model. Species sequenced in the present study are shown in bold type. The numbers near branches are ML bootstrap values/Bayesian inference (BI) posterior probability values. The scale bar corresponds to five substitutions per 100 nucleotide positions.

DISCUSSION

Morphology comparison (Table 3)

Pseudoamphisiella elongata sp. nov. can be easily distinguished from the other three species of *Pseudoamphisiella*, i.e. *P. lacazei*, *P. alveolata*, and *P. quadrinucleata*, by its extremely elongate–slender body shape (vs. elongate–oval in other *Pseudoamphisiella* species), fewer dorsal kineties (six or seven in *P. elongata* sp. nov. vs. around ten or more in other species), fewer caudal cirri (six or seven in *P. elongata* sp. nov. vs. ten or more in other species), more marginal cirri (on average 39 left and 31 right marginal row cirri in *P. elongata* sp. nov. vs. fewer than 30 in other species), and differentiated pretransverse cirri (vs. pretansverse cirri absent in other species). Moreover, as regards the number of macronuclear nodules, *P. elongata* sp. nov. can be easily separated from *P. alveolata* and *P. quadrinucleata* (25–44 vs. invariably two in *P. alveolata* and four in *P. quadrinucleata*) (Table 3; Shao *et al.*, 2006; Song, 1996; Song *et al.*, 1997; Song & Warren, 2000; Shen *et al.*, 2008).

Significantly, the separation of *Pseudoamphisiella* spp. is also firmly supported by the SSU rRNA gene sequence data, which demonstrate that there is a considerable evolutionary distance between the known species and the new form (Fig. 7A; Table 2).

Apart from its congeners, the most similar species to *P. elongata* sp. nov. is *Leptoamphisiella vermis* (Gruber, 1888) Li *et al.*, 2007, with which it shares a number of morphological similarities, i.e. the elongated body shape, the narrow, cephalized buccal field, the colour of the cytoplasm, the conspicuous alveolar layer with rod-like extrusomes, and the general ciliary pattern. Nevertheless, the two can easily be separated by: (1) the body size *in vivo* (400–1000 μm × 40–70 μm in *L. vermis* vs. 160–240 μm × 30–40 μm in *P. elongata* sp. nov.); (2) the contractility of the cell (high vs. inconspicuous); (3) caudal cirri (absent vs. present); (4) the number of transverse cirri (52–80 vs. 16–21); (5) the number of dorsal kineties (9–13 vs. 6 or 7) (Li *et al.*, 2007).

It is noteworthy that an illustration of an American population of *P. lacazei* by Borror & Wicklow (1983)

Table 3. Morphometric comparison of *Pseudoamphisiella elongata* sp. nov. with *P. quadrinucleata* Shen *et al.*, 2008, *P. lacazei* (Maupas, 1883) Song, 1996 and *P. alveolata* (Kahl, 1932) Song & Warren, 2000

Character	*P. elongata*	*P. quadrinucleata*	*P. lacazei*	*P. alveolata*
Body size *in vivo*	160–240 × 30–40	160–220 × 60–100	120–240 × 50–80	120–300 × 40–80
Macronuclear nodules	25–44 ($N = 29$)	4 ($N = 43$)	24–57 ($N = 20$)	2 ($N = 16$)
Micronuclei	6–17 ($N = 23$)	2–6 ($N = 36$)	7–10 ($N = 6$)	2–5 ($N = 11$)
Adoral membranelles	39–49 ($N = 30$)	49–75 ($N = 37$)	39–49 ($N = 25$)	47–59 ($N = 9$)
Buccal cirri	2 ($N = 30$)	2–3 ($N = 40$)	2 ($N = 25$)	2 ($N = 18$)
Frontal cirri	3 ($N = 29$)	3 ($N = 41$)	3 ($N = 25$)	3 ($N = 18$)
Left midventral cirri	13–17 ($N = 29$)	11–22 ($N = 35$)	16–23 ($N = 26$)	10–14 ($N = 11$)
Right midventral cirri	15–21 ($N = 29$)	14–20 ($N = 37$)	11–16 ($N = 26$)	11–15 ($N = 11$)
Left marginal cirri	26–45 ($N = 28$)	15–31 ($N = 39$)	21–34 ($N = 16$)	14–20 ($N = 11$)
Right marginal cirri	28–36 ($N = 28$)	14–20 ($N = 33$)	20–31 ($N = 16$)	12–14 ($N = 11$)
Transverse cirri	16–21 ($N = 29$)	14–23 ($N = 40$)	16–23 ($N = 26$)	12–16 ($N = 16$)
Pretransverse cirri	2–3 ($N = 24$)	Absent	Absent	Absent
Caudal cirri	6–7 ($N = 27$)	13–24 ($N = 40$)	9–11 ($N = 5$)	11–16 ($N = 9$)
Dorsal kineties	6–7 ($N = 28$)	12–17 ($N = 25$)	8–11 ($N = 25$)	10–12 ($N = 16$)
Alveolar layer	Present	Present	Inconspicuous	Present
Data source	Present work	Shen *et al.* (2008)	Song (1996)	Song & Warren (2000)

resembles *P. elongata* sp. nov. in body size and shape, narrow buccal field, general arrangement of cirri, and number of macronuclear nodules (Borror & Wicklow, 1983; Berger, 2006). A reinvestigation of this organism based on observations of living and protargol-impregnated specimens is required, however, before any conclusion can be made concerning its true identity.

Divisional morphogenesis and systematic position

Morphogenesis has previously been reported for two species of *Pseudoamphisiella*, namely: *P. lacazei* (the type species) and *P. alveolata* (Song *et al.*, 1997; Shao *et al.*, 2006). Song *et al.* (1997) established the family Pseudoamphisiellidae based largely on the morphogenetic features of *P. lacazei*. Subsequently, the entire morphogenetic processes of Japanese and Chinese populations of *P. alveolata* were reported, enabling the analysis of the phylogenetic position of the family Pseudoamphisiellidae to be ascertained (Hu & Suzuki, 2006; Shao *et al.*, 2006).

The three species of *Pseudoamphisiella* for which morphogenetic processes have been investigated share several features, including: the oral primordium in the opisthe and the FVT-anlagen in both dividers are formed independently; the left marginal row and dorsal kineties develop within the old structures; a single caudal cirrus develops from the posterior end of each dorsal kinety; the FVT-anlagen give rise to the frontal cirri, buccal cirri, two widely separated midventral rows, and a row of well-developed transverse cirri; the macronuclear nodules will fuse into a single mass before division. In addition, *P. elongata* sp. nov. share two morphogenetic features with the morphologically similar *P. lacazei*: namely that the old oral apparatus is completely replaced, and the right marginal row anlagen develop independently. There are, however, a number of minor differences between them including: (1) one 'extra' anlage is generated, which then develops into two or three 'extra' marginal cirri that connect the caudal and the marginal cirral rows (vs. extra cirri absent in *P. lacazei*); (2) the last FVT-streak contributes the two anteriormost cirri to form migratory cirri (frontoterminal cirri), which may eventually be resorbed (vs. migratory cirri not formed in *P. lacazei*); (3) the OP develops in the outermost region of the cortex in *P. elongata* sp. nov. (vs. OP develops beneath the cortex in *P. lacazei*); (4) the FVT anlagen develop in a secondary mode. It should be noted, however, that the second and the third dissimilarities may simply be a result of lack of data for *P. lacazei*, for which the morphogenetic process has not been described in full. Furthermore, the origin of the RMA in *P. elongata* sp. nov. is similar to that illustrated by Song *et al.* (1997) for *P. lacazei*. A reinvestigation of morphogenesis in *P. lacazei* is therefore needed in order to ascertain whether there are any significant differences with that in *P. elongata* sp. nov.

In addition to the general morphogenetic features of *Pseudoamphisiella*, *P. alveolata* and *P. elongata* sp. nov. also share a number of features, including: the OP develops in the outermost region of the cortex; the FVT-anlagen develop in a primary mode; an 'extra'

marginal anlage originates to the right of the RMA, and develops into two or three 'extra' marginal cirri. Morphogenesis in *P. elongata* sp. nov. differs from *P. alveolata* as follows: (1) the OP develops *de novo*, and the old AZM is completely renewed (vs. only partly renewed in *P. alveolata*); (2) the last FVT-streak contributes two migratory cirri (frontoterminal cirri), which may ultimately be resorbed (vs. migratory cirri not produced in *P. alveolata*); (3) the RMA originates independently from the old structure (vs. RMA develops within the old structure in *P. alveolata*).

Thus, from the present and previous studies on *Pseudoamphisiella*, three different patterns of morphogenesis can be recognized: (1) oral apparatus completely renewed and formation of FVT-anlagen achieved by primary mode (*P. elongata* sp. nov.); (2) oral apparatus completely renewed and formation of FVT-analgen achieved by secondary mode (*P. lazcazei*); (3) oral apparatus partly renewed and formation of FVT-anlagen achieved by primary mode (*P. aveolata*).

The phylogenetic assignment of pseudoamphisiellids remains unclear, although Berger (2006) tentatively placed them in the family Holostichidae. According to Shao *et al.* (2006), the family Pseudoamphisiellidae should be assigned to the order Urostylida, based on the basic pattern of development of ciliature in *P. alveolata*. The appearance of migratory cirri (i.e. frontoterminal cirri) during morphogenesis in *P. elongata* sp. nov. and in other congeners offers further support for this placement (Song *et al.*, 1997; Hu & Suzuki, 2006; Shao *et al.*, 2006). This hypothesis, however, was challenged by molecular data based on SSU rRNA gene sequence analysis (Yi *et al.*, 2008), which indicates that the pseudoamphisiellids should be separated from the urostylids and placed in a group yet to be defined that includes both Pseudoamphisiellidae and the discocephalines. This suggestion is supported by other recent studies performed by Zhenzhen Yi in the same laboratory as the senior author in the OUC (Z. Yi, unpubl. data, pers. comm.), based on morphogenetic and molecular data analyses, respectively. According to the current information available, we agree with Yi *et al.* (2008) that the pseudoamphisiellids should be treated as incertae sedis until further data are available.

ACKNOWLEDGEMENTS

This work was supported by the Natural Science Foundation of China (project numbers: 4067607 and 30870264), the Darwin Initiative Programme (project number: 14-015), which is funded by the UK Department of Environment, Food, and Rural Affairs, and a grant from the Center of Excellence in Biodiversity, King Saud University. We also thank Prof. Xiaozhong Hu and Dr. Chen Shao, OUC, for their help in preparing the draft.

REFERENCES

Berger H. 2006. Monograph of the Urostyloidea (Ciliophora, Hypotricha). *Monographiae Biologicae* **85:** 1–1303.

Borror AC, Wicklow BJ. 1983. The suborder Urostylina Jankowski, (Ciliophora, Hypotrichida): morphology, systematics and identification of species. *Acta Protozoologica* **22:** 97–126.

Felsenstein J. 1995. '*PHYLIP: phylogeny inference package*'. 3.57c edn. Seattle, WA: Department of Genetics, University of Washington.

Hu X, Suzuki T. 2006. Observation on a Japanese population of *Pseudoamphisiella alveolata* (Kahl, 1932) Song & Warren, 2000 (Ciliophora: Hypotrichida): morphology and morphogenesis. *Acta Protozoologica* **45:** 41–52.

Kimura M. 1980. A simple method of estimating evolutionary rates of base substitutions through comparative studies of nucleotide sequences. *Journal of Molecular Evolution* **16:** 111–120.

Li L, Song W, Al-Rasheid KA, Hu X, Al-Quraishy SA. 2007. Redescription of a poorly known marine ciliate, *Leptoamphisiella vermis* Gruber, 1888 n. g., n. comb. (Ciliophora, Stichotrichia, Pseudoamphisiellidae), from the Yellow Sea, China. *Journal of Eukaryotic Microbiology* **54:** 527–534.

Li L, Song W, Warren A, Al-Rasheid KA, Roberts D, Yi Z, Al-Farraj SA, Hu X. 2008. Morphology and morphogenesis of a new marine ciliate, *Apokeronopsis bergeri* nov. spec. (Ciliophora, Hypotrichida) from the Yellow Sea, China. *European Journal of Protistology* **44:** 208–219.

Lin X, Li J, Gong J, Warren A, Song W. 2008. Taxonomic studies on three marine pleurostomatid ciliates, *Litonotus bergeri* nov. spec., *L. blattereri* nov. spec. and *L. petzi* nov. spec. (Ciliophora, Pleurostomatida) from north China sea. *European Journal of Protistology* **44:** 91–102.

Lynn DH, Small EB. 2002. Phylum Ciliophora Doflein, 1901. In: Lee JJ, Leedale GG, Bradbury PC, eds. *The illustrated guide to the protozoa*, 2nd edn. Lawrence, KS: Allen Press Inc., 371–656.

Shang H, Song W, Warren A. 2003. Phylogenetic positions of two ciliates, *Paranophrys magna* and *Mesanophrys carcini* (Ciliophora: Oligohymenophorea), within the subclass Scuticociliatia inferred from complete small subunit rRNA gene sequences. *Acta Protozoologica* **42:** 171–181.

Shao C, Song W, Warren A, Al-Rasheid KA, Yi Z, Gong J. 2006. Morphogenesis of the marine ciliate *Pseudoamphisiella alveolata* (Kahl, 1932) Song & Warren, 2000 (Ciliophora, Stichotrichia, Urostylida) during binary fission. *Journal of Eukaryotic Microbiology* **53:** 388–396.

Shen Z, Lin X, Long H, Miao M, Liu H, Al-Rasheid KA, Song W. 2008. Morphology and SSU rDNA gene sequence of *Pseudoamphisiella quadrinucleata* n. sp. (Ciliophora, Urostylida) from the South China Sea. *Journal of Eukaryotic Microbiology* **55:** 510–514.

Song W. 1996. Description of the marine ciliate *Pseudoamphisiella lacazei* (Maupas, 1883) nov. gen., nov. comb. (Protozoa, Ciliophora, Hypotrichida). *Oceanologia et Limnologia Sinica* **27:** 18–22 (in Chinese with English summary).

Song W, Warren A. 2000. *Pseudoamphisiella alveolata* (Kahl, 1932) nov. comb., a large marine hypotrichous ciliate from China (Protozoa, Ciliophora, Hypotrichida). *European Journal of Protistology* **36:** 451–457.

Song W, Warren A, Hu X. 1997. Morphology and morphogenesis of *Pseudoamphisiella lacazei* (Maupas, 1883) Song, 1996 with suggestion of establishment of a new family Pseudoamphisiellidae nov. fam. (Ciliophora, Hypotrichida). *Archiv fur Protistenkunde* **147:** 265–276.

Wilbert N. 1975. Eine verbesserte Technik der Protargolimprägnation für Ciliaten. *Mikrokosmos* **64:** 171–179.

Yi Z, Song W, Warren A, Roberts D, Al-Rasheid K, Chen Z, Al-Farraj S, Hu X. 2008. A molecular phylogenetic investigation of *Pseudoamphisiella* and *Parabirojimia* (Protozoa, Ciliophora, Spirotrichea), two genera with ambiguous systematic positions. *European Journal of Protistology* **44:** 45–53.